Coordination Chemistry Reviews
190–192 (1999) 961–974

COORDINATION CHEMISTRY REVIEWS

www.elsevier.com/locate/ccr

New approach to the construction of an artificial hemoprotein complex

Takashi Hayashi [a,b,*], Yutaka Hitomi [b], Tetsuo Takimura [b], Atsushi Tomokuni [b], Tadashi Mizutani [b], Yoshio Hisaeda [a], Hisanobu Ogoshi [b,c]

[a] *Department of Chemistry and Biochemistry, Graduate School of Engineering, Kyushu University, Fukuoka 812-8581, Japan*
[b] *Department of Synthetic Chemistry and Biological Chemistry, Graduate School of Engineering, Kyoto University, Kyoto 606-8501, Japan*
[c] *Fukui National College of Technology, Sabae 916-8507, Japan*

Accepted 6 April 1999

Contents

* Corresponding author. Present address: Kyushu University. Tel.: +81-92-642-3595; fax: +81-92-632-4718.
E-mail address: thayatcm@mbox.nc.kyushu-u.ac.jp (T. Hayashi)

PII: S0010-8545(99)00131-9

Abstract

Modified prosthetic metalloporphyrin, having a total of eight carboxylate groups at the terminal of two peripheral propionate side chains, was inserted into apomyoglobin to yield a new reconstituted myoglobin. The cluster of substituted carboxylates acts as the binding domain for cationic compounds such as methyl viologen and cytochrome *c*. Fluorescence spectroscopic analysis indicates that the reconstituted myoglobin formed a stable complex with methyl viologen and photoinduced singlet electron transfer (ET) occurred within the complex; $k_{et} = 2.1 \times 10^9\ s^{-1}$ and $k_{cr} = 3.3 \times 10^8\ s^{-1}$. Cytochrome *c* with a positively charged domain also interacted with the reconstituted myoglobin with an association constant of $6.5 \times 10^4\ M^{-1}$. The photoinduced triplet ET from the zinc reconstituted myoglobin to ferricytochrome *c* occurred through diprotein complex with a rate constant of $2.2 \times 10^3\ s^{-1}$. Furthermore, compared to native myoglobin, the ferryl state of the reconstituted myoglobin generated by hydrogen peroxide revealed the peroxidase activity with the acceleration of the oxidation of ferrocytochrome *c* via complex formation. The present approach could be very useful for constructing practical protein–protein complex systems to elucidate the biological ET via noncovalently linked biomolecules.

Keywords: Reconstituted myoglobin; Molecular recognition; Cytochrome *c*; Methyl viologen; Electron transfer; Peroxidase activity

1. Introduction

Electron transfer (ET) reactions in metalloprotein assembly are crucial to a wide range of enzymatic processes in both photosynthesis and respiratory oxidative phosphorylation. In these systems, there are several elaborate ET cascades, where electrons are transferred within protein–protein or protein–cofactor complex formed by specific interaction. In the last decade, it has been well known that the metalloproteins have a unique binding domain on the protein surface and recognize their redox partners [1]. For example, cytochrome *c*, which is a mobile heme protein with highly positive charge due to a total of 19 lysine amino groups, is located in mitochondria in order to shuttle between several oxidoreductases such as the cytochrome bc_1 complex, cytochrome oxidase, cytochrome b_5, and transfer an electron. Recent work focusing on the binding behavior of cytochrome *c* indicates that special lysine amino groups on the front of the heme pocket act as a cationic binding site for an anionic receptor domain of the redox partners. In fact, the X-ray crystal structure of cytochrome *c* oxidase suggests that there are several acidic amino acids located in the cytochrome *c* binding sites [2]. Therefore, it is of particular interest to demonstrate the importance of protein–protein or protein–cofactor recognition in a long-range ET process by use of a highly ordered supramolecular model system in conjunction with a native protein system.

Recently, we have reported a new approach to the construction of an anionic binding domain on the surface of myoglobin by use of the reconstitutional technique with a functionalized heme [3], which enabled us to obtain the electrostatic self-associated complex between the reconstituted myoglobin and methyl viologen or cytochrome *c* based on electrostatic interaction. In this review, we wish

to present new ET systems in the self-associated complexes through molecular recognition events on the protein surface.

2. New strategy for the construction of binding domains on the protein surface

Myoglobin is an oxygen storage protein and is well characterized in terms of both primary and tertiary structures, in which protoporphyrin IX iron complex (heme) as a prosthetic group contacts the peptide matrix of the protein via multiple weak interactions. One of the significant characteristics is that the native prosthetic group can be replaced with an artificial metalloporphyrin by the usual reconstitutional techniques [4]. Thus, a reconstituted myoglobin is easily obtained by the insertion of a heme analog into apomyoglobin as shown in Scheme 1. In the last decade, we have studied the structure and reactivity of a myoglobin reconstituted with the synthetic hemin conjugated with several functional groups at the terminal of peripheral propionate side chain through an amide linkage [5]. The observation indicated that the replacement of a propionate in the hemin with a propionamide has no serious effect on the structure and stability of the protein.

This information encouraged us to construct a cytochrome *c* receptor by a myoglobin reconstituted with a synthetic porphyrin. To mimic the oxidoreductase as a partner of cytochrome *c*, we have recently prepared the synthetic porphyrin having multiple anionic charged functions at the terminal of two propionates and inserted it into apomyoglobin to yield the functionalized myoglobin. One of the principal advantages in this method is that a specific interface can be localized on the protein surface. Here, we will demonstrate an artificial protein–cofactor and protein–protein interactions by use of the reconstitution strategy.

3. Complex formation between zinc myoglobin and methyl viologen

3.1. Binding of methyl viologen to the artificial domain of the myoglobin surface

In the first stage, we have prepared a reconstituted myoglobin, rMb(**1**·Zn), and monitored the interaction with methyl viologen dication (MV) as shown in Scheme 1 [6]. Zinc porphyrin **1** has a total of eight carboxylates bound to the terminal of

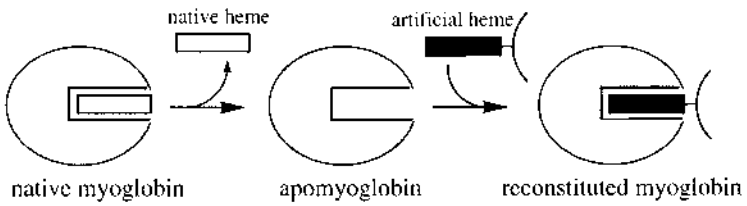

Scheme 1.

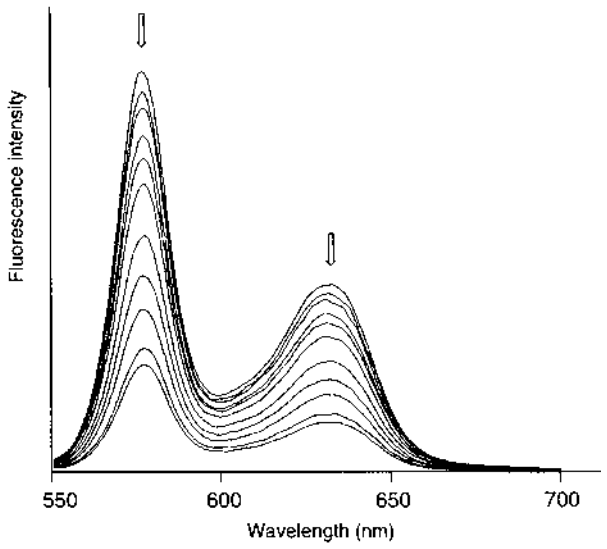

Fig. 1. Fluorescence spectral changes upon addition of 0–500 equivalents of MV to rMb(**1**·Zn) solution (2.0×10^{-6} M) in pH 7.0, 10 mM phosphate buffer at 25°C; excitation at 543 nm.

two peripheral propionate side chains. The reconstitution from **1**·Zn and apomyoglobin proceeded smoothly. The characteristic visible absorption and CD spectra of the reconstituted protein were similar to those of reference protein rMb(**2**·Zn) reconstituted with mesoporphyrin zinc complex (**2**·Zn), suggesting that the artificial prosthetic group was inserted into the normal position of the heme pocket. Furthermore, the isoelectric point of rMb(**1**·Zn) was determined to be 5.6 ± 0.2, which is about 1.3 pH units lower than that of rMb(**2**·Zn). Thus, the reconstituted myoglobin converts neutral protein to the acidic protein due to the substitution of eight carboxylates at the terminal of peripheral propionates.

Fig. 1 reveals that fluorescence emission at 580 and 635 nm from the zinc porphyrin in rMb(**1**·Zn) was quenched upon addition of MV. Stern–Volmer plots in Fig. 2 indicate that static quenching is observed at lower concentration of MV ([MV] < 0.01 M) in phosphate buffer (10 mM, pH 7.0). Thus, the static quenching occurs due to photoinduced singlet ET from rMb(**1**·Zn) to MV at lower concentrations of MV. Furthermore, the quenching efficiency increased with the increase of pH value and decreased with the increase of ionic strength, suggesting that rMb(**1**·Zn) associates with MV through the artificial carboxylate interface. In contrast, fluorescence from **2**·Zn in the protein was not quenched even at a MV concentration of 0.01 M. These results indicate that the ground-state complex between rMb(**1**·Zn) and MV is formed by electrostatic interaction as shown in Scheme 2.

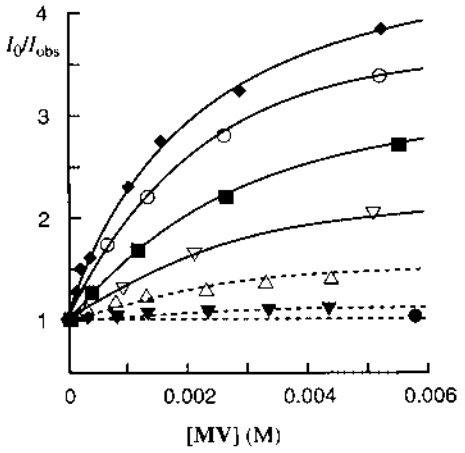

Fig. 2. Stern–Volmer plots for the fluorescence quenching of zinc porphyrin in the myoglobin upon addition of MV at 10 mM phosphate buffer at 25°C. The solid lines correspond to the data obtained in rMb(**1**·Zn): pH 5.8 (▽); pH 6.1 (■); pH 6.4 (○); pH 7.1 (◆). [rMb(**1**·Zn)] = 10^{-6} M. The dashed lines correspond to the data obtained in rMb(**2**·Zn): pH 7.0 (●); rMb(**3**·Zn): pH 7.0 (▼); rMb(**4**·Zn): pH 7.0 (△). [rMb(**2**·Zn)] = [rMb(**3**·Zn)] = [rMb(**4**·Zn)] = 10^{-6} M. The changes of fluorescence emission were monitored at 584 nm (λ_{ex} = 543 nm).

3.2. Evaluation of the artificial binding domain on the protein surface

To investigate the structural basis of interfacial recognition between the reconstituted myoglobin and MV on the protein surface, we have further prepared the reconstituted proteins rMb(**3**·Zn) and rMb(**4**·Zn) as shown in Scheme 3 [7]. Zinc

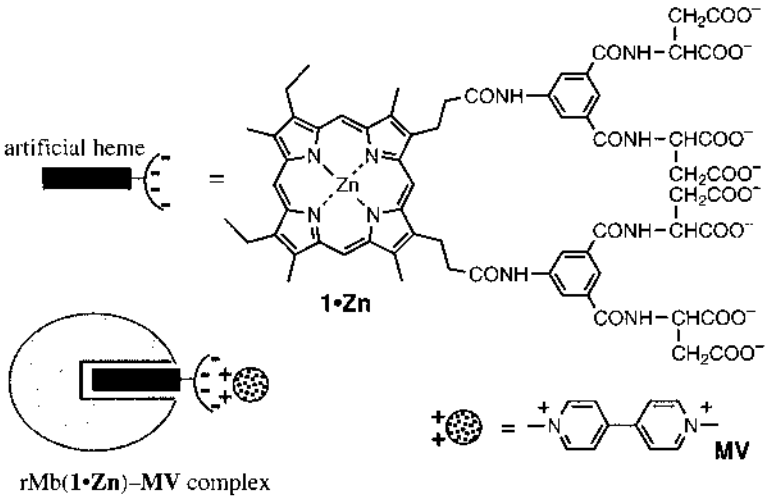

Scheme 2.

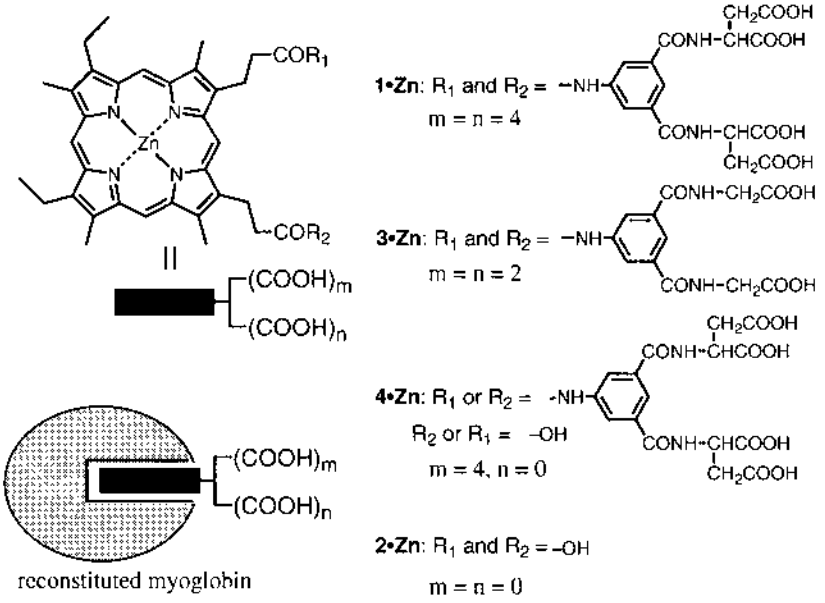

Scheme 3.

porphyrins **3**·Zn and **4**·Zn have a total of four carboxylate groups [(2 + 2) and (4 + 0) binding sites bound to the terminal of the propionate side chains]. Fig. 2 also shows the Stern–Volmer plots to compare the quenching efficiency in these systems. Interestingly, the fluorescence emissions of rMb(**3**·Zn) and rMb(**4**·Zn) were hardly quenched by MV. Thus, the anionic charges of the binding domain on the surface of rMb(**3**·Zn) and rMb(**4**·Zn) is not enough to bind MV. In fact, the X-ray crystal structure analysis of native myoglobin from horse heart suggests that there are several cationic amino groups (Lys45, Lys63 and Lys96) located on the heme pocket edge as shown in Fig. 3 [8], which should associate with some of the carboxylates and inhibit the interaction between the carboxylate binding domain and MV. Therefore, the stable complexation between the myoglobin and MV requires the localized carboxylate cluster formed by more than four carboxylate groups.

3.3. Photoinduced singlet ET from the zinc myoglobin to methyl viologen

Time-resolved fluorescence studies indicated that the decay profiles of rMb(**1**·Zn), initially single exponential with $\tau = 2.0 \pm 0.1$ ns, became biphasic upon addition of MV; $\tau_L = 2.0 \pm 0.1$ and $\tau_S = 0.4 \pm 0.1$ ns, respectively. The longer and shorter lived components of the biphasic decay curve are assignable to free rMb(**1**·Zn) and rMb(**1**·Zn)–MV complexes, respectively. Table 1 summarizes the fluorescence lifetimes and the relative magnitudes in different concentrations of MV. The derived fluorescence lifetimes were independent of concentration of MV, whereas

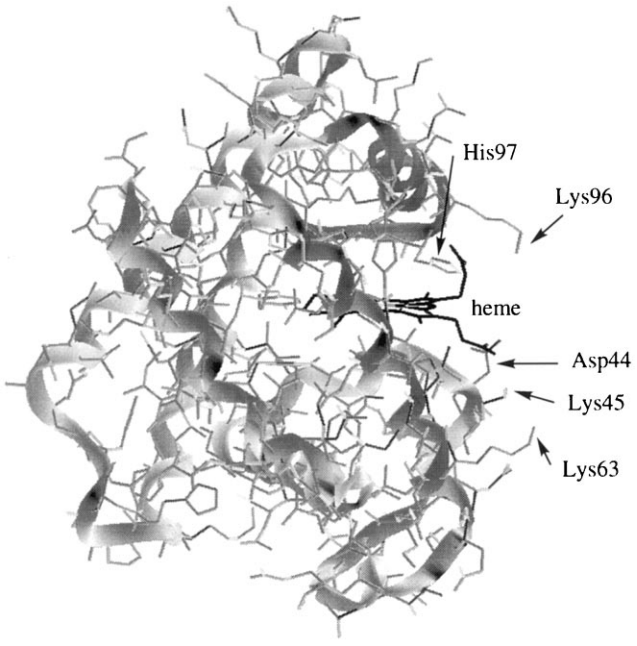

Fig. 3. Structure of native horse heart metmyoglobin, based on the Brayer's coordination [8].

the fractional contribution of the shorter component, A_S, increased with the increase of the concentration of MV, suggesting the complex formation between the protein and MV. A rate constant of forward singlet ET was determined to be $2.1 \times 10^9\ s^{-1}$, which was derived as the following equation: $k_{et} = 1/\tau_S - 1/\tau_L$.

Picosecond laser flash photolysis studies by a streak camera exhibited the characteristic transient absorption spectra of rMb(**1**·Zn) in the presence of excess MV, in which a strong absorption band centered at 455 nm can be assigned to the superposition of excited singlet and triplet excited states and cation radical species

Table 1
Fluorescence lifetimes of rMb(**1**·Zn) in the presence of MV[a]

Concentration			
rMb(**1**·Zn) (M)	MV (M)	τ_S (ns) [b,c]	τ_L (ns) [b,c]
3.5×10^{-6}	0		2.0 (100%)
3.4×10^{-6}	2.1×10^{-4}	0.5 (26%)	2.1 (74%)
2.8×10^{-6}	1.1×10^{-3}	0.4 (50%)	2.0 (50%)
2.8×10^{-6}	1.4×10^{-2}	0.4 (76%)	1.8 (24%)

[a] In the aqueous phosphate buffer (10 mM) pH 7.0 at 25°C.
[b] Numbers in parentheses are exponential factors; A_S and A_L.
[c] Estimated errors are <0.1 ns.

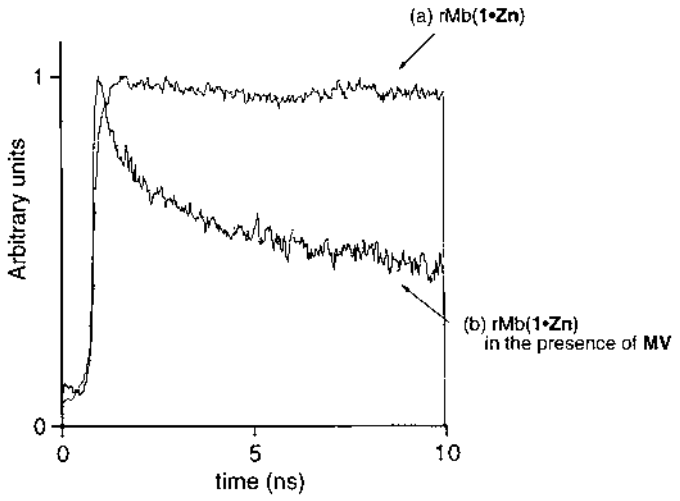

Fig. 4. Transient absorbance changes for data obtained at 447–462 nm. (a) rMb(**1**·Zn) and (b) rMb(**1**·Zn) in the presence of MV in pH 7.0, 10 mM phosphate buffer at 25°C. $[\mathrm{rMb}(\mathbf{1}\cdot\mathrm{Zn})] = 6.0 \times 10^{-4}$ M, $[\mathrm{MV}] = 2.7 \times 10^{-2}$ M.

of **1**·Zn in the protein. Absorption changes observed at 447–462 nm for rMb(**1**·Zn) are shown in Fig. 4, where the clear decay was found in the presence of a large excess of MV. In contrast, there is no time dependence of this change in the absence of the electron acceptor MV. These data are direct evidence for singlet ET from rMb(**1**·Zn) to MV. The photoinduced ET process of rMb(**1**·Zn)–MV system after laser flash is represented in Scheme 4, where the absorbance decay profile of three transient species in the presence of MV can be fitted to the integrated form of the following equations [9]:

$$\mathrm{d}[^{*1}\mathrm{P{-}MV}]/\mathrm{d}t = -(1/\tau_1)[^{*1}\mathrm{P{-}MV}] \quad (1)$$

$$\tau_1 = 1/(k_{\mathrm{et}} + k_{\mathrm{isc}} + k_{\mathrm{ic}} + k_{\mathrm{f}})$$

$$\mathrm{d}[^{+}\mathrm{P{-}MV}^{-}]/\mathrm{d}t = k_{\mathrm{et}}[^{*1}\mathrm{P{-}MV}] - (1/\tau_2)[^{+}\mathrm{P{-}MV}^{-}] \quad (2)$$

$$\tau_2 = 1/k_{\mathrm{cr}}$$

$$\mathrm{d}[^{*3}\mathrm{P{-}MV}^{-}]/\mathrm{d}t = k_{\mathrm{isc}}[^{*1}\mathrm{P{-}MV}] \quad (3)$$

$$\Delta A_{447-462} = \Delta\varepsilon_{*1\mathrm{P-M}}\mathrm{V}[^{*1}\mathrm{P{-}MV}] + \Delta\varepsilon_{+\mathrm{P-MV}-}[^{+}\mathrm{P{-}MV}^{-}] + \Delta\varepsilon_{*3\mathrm{P-MV}}[^{*3}\mathrm{P{-}MV}] \quad (4)$$

From fitting of the decay curve in Fig. 3 by use of Eq. (4), the values of τ_1 and τ_2 can be determined as 0.31 ± 0.1 and 3.3 ± 0.2 ns, respectively ($r^2 = 0.97$). The former value τ_1 is consistent with τ_S determined by fluorescence lifetime measurement, and this agreement demonstrates the reliability of experimental data and evaluated value, $k_{\mathrm{et}} = 2.1 \times 10^9$ s^{-1}. The latter value τ_2 indicates the degree of charge recombination of cation radical species, thermal back ET, with a rate constant of $k_{\mathrm{cr}} = 3.3 \times 10^8$ s^{-1}.

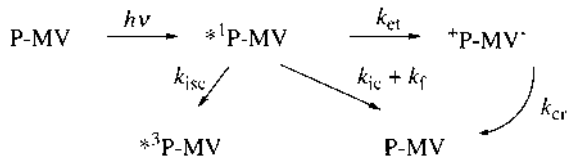

*1P : singlet excited zinc porphyrin in the protein
*3P : triplet excited zinc porphyrin in the protein
+P : zinc porphyrin cation radical species in the protein

Scheme 4.

In contrast, the transient absorption spectra for rMb(**2**·Zn) in the presence of MV show no clear decay of absorption in the same time range. Although the photoinduced ET from triplet excited state of zinc myoglobin to MV occurs through diffusion-controlled [10], no such singlet ET reaction has been reported for zinc myoglobin. To our knowledge, the present work is the first example of a singlet ET within the stable complex between the zinc myoglobin and electron acceptor.

4. Artificial diprotein complex—a reconstituted myoglobin and cytochrome *c*

4.1. Design of cytochrome c receptor by use of the reconstituted myoglobin

It is well known that the special positively charged patch formed by several lysine groups on the edge of the cytochrome *c* heme pocket is used for the interaction with all of the redox partners in the mitochondrial respiratory system. Therefore, to mimic the cytochrome *c* receptor, we have prepared the second-generation proteins, rMb(**5**·Zn) and rMb(**5**·Fe) having an anionic binding interface on the protein surface as shown in Scheme 5 [11,12]. Porphyrin **5**, which has a total of eight carboxylate groups at the terminal of propionate side chains, was synthesized from the coupling of protoporphyrin IX **6** and 5-aminoisophthalic acid derivative. The metalloporphyrins, **5**·Zn and **5**·Fe, were readily inserted into apomyoglobin to give the reconstituted proteins, rMb(**5**·Zn) and rMb(**5**·Fe), respectively. The stability and characteristic UV–vis, CD and NMR spectra of the myoglobins were comparable to those of the reference proteins, rMb(**6**·Zn) reconstituted with protoporphyrin IX zinc complex and native Mb(**6**·Fe), respectively. Isoelectric focusing was carried out for rMb(**5**·Fe) and native Mb(**6**·Fe). The isoelectric point, p*I*, of the meta -quo form of rMb(**5**·Fe) is 5.5, which is about 2 pH units lower than that of native Mb(**6**·Fe), suggesting the reconstituted myoglobin converted the neutral protein to acidic protein due to the construction of anionic cluster as an interface.

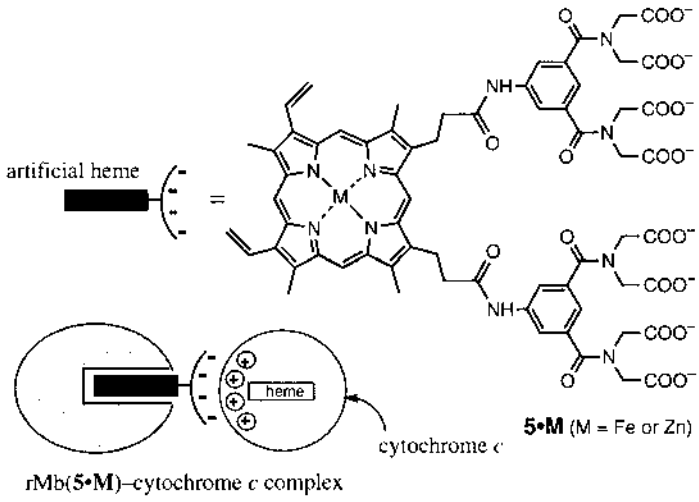

Scheme 5.

4.2. NMR monitoring of protein–protein complexation

The binding behavior of rMb(**5**·Fe) and cytochrome *c* was supported by a ^{1}H NMR titration experiment. The characteristic paramagnetic shifts of heme 1-CH_3, 5-CH_3 and Ile99 CγH of rMb(**5**·Fe) in the presence of CN^- appeared at 19.2, 25.2 and -8.0 ppm, respectively. Upon addition of ferricytochrome *c* to the myoglobin solution, these resonances were changed as a function of increasing concentration of cytochrome *c*; particularly heme 5-CH_3 resonance of rMb(**5**·Fe) shifted upfield ($\Delta\delta = -0.4$ ppm at three equivalents of cytochrome *c*). The heme 3-CH_3 and 8-CH_3 resonances of ferricytochrome *c* also shifted from their original positions, whereas Met80 CεH_3 protons only deviated about 0.02 ppm. The direction and the size of the shifts are similar to those seen in the titrimetric measurement by use of cytochrome *c* and cytochrome *c* peroxidase [13]. Thus, the complex structure of rMb(**5**·Fe) and cytochrome *c* would be similar to that of the native complex between cytochrome *c* peroxidase and cytochrome *c*. The anticipated complex is shown in Fig. 5, a computer-generated composite of the crystal structure of horse heart metmyoglobin [8] and cytochrome *c* [14].

4.3. Photoinduced ET from zinc myoglobin to cytochrome c within the protein complex

The photoinduced ET reactions between rMb(**5**·Zn) and cytochrome *c* were followed by monitoring the decay of the triplet excited state of the zinc porphyrin at 460 nm. The decay in the protein with a rate constant of 59 ± 1 s^{-1} was almost same as that for rMb(**6**·Zn) at pH 7.0. Furthermore, addition of ferrocytochrome *c* gave no remarkable changes in the triplet decay of rMb(**5**·Zn). In contrast, upon

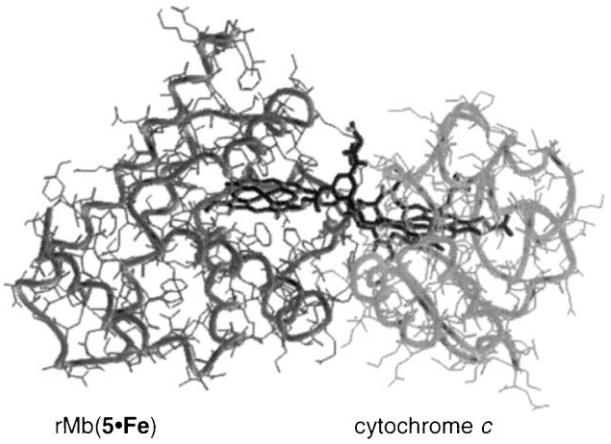

Fig. 5. Hypothetical structure of rMb(**5**·Fe)–cytochrome *c* complex. The structure shown is a composite of the crystal structure of horse heart metmyoglobin (left protein) [8] and cytochrome *c* (right protein) [14] that emerged from the plausible interactions between carboxylate interface in rMb(**5**·Fe) and special lysine residues of cytochrome *c*.

addition of ferricytochrome *c*, the triplet excited state of rMb(**5**·Zn) was rapidly quenched at the ionic strength of 10 or 20 mM (pH 7.0) as shown in Fig. 6, indicating that the photoinduced ET reaction from rMb(**5**·Zn) to ferricytochrome *c* occurs within the diprotein complex. The decay rate of the triplet excited state

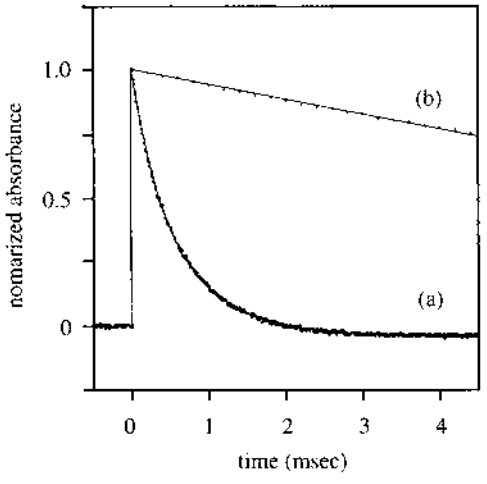

Fig. 6. Transient absorption changes for rMb(**5**·Zn) at 460 nm after laser flash. (a) Triplet decay of rMb(**5**·Zn) in the presence of cytochrome *c*. $[rMb(\mathbf{5}\cdot Zn)] = 4.3 \times 10^{-6}$ M, [cytochrome *c*] $= 1.6 \times 10^{-5}$ M in 5 mM phosphate buffer at pH 7.0. (b) Triplet decay of rMb(**5**·Zn) in the absence of cytochrome *c*. Experimental data points are represented by dots; the solid lines are fitting curves using a single-exponential function.

decreased with the increase of ionic strength in the presence of ferricytochrome *c*, indicating that the diprotein complex was formed through electrostatic interaction. Furthermore, two short-lived transient bands appeared at 680 and 550 nm, which are representative of the zinc porphyrin cation radical species and ferrocytochrome *c*, respectively, as an intermediate of ET. These transient bands increased with the decay of triplet excited states of rMb(**5**·Zn) and subsequently decreased in a longer time scale through thermal back ET process.

The decay curve can be fitted by a single exponential function to give a rate constant k_{obs}, which is dependent on the concentration of cytochrome *c*. The binding affinity K_a and the rate constant of forward ET k_{et} were determined by k_{obs}; $k_{obs} = k_0 + k_{et}{:}f$, where k_0 and f represent the rate constants of triplet-state decay in the absence of cytochrome *c* and the fraction of complexed rMb(**5**·Zn). From the curve-fitting analysis in different concentrations of cytochrome *c*, the binding affinity and rate constant were determined to be $(6.5 \pm 3.0) \times 10^4$ M^{-1} and $(2.2 \pm 0.1) \times 10^3$ s^{-1}, respectively, at 10 mM ionic strength (pH 7.0). Compared to the kinetic and binding behavior of interprotein ET system in the previous literature [15,16], the present data seem to be reasonable. Construction of a variety of artificial protein–protein complexes by use of different binding domain and exploration of these interprotein ET are in progress.

4.4. Cytochrome c peroxidase activity of the reconstituted myoglobin

It is well-known that cytochrome *c* peroxidase which catalyzes the oxidation of ferrocytochrome *c* has a specific binding domain on the protein surface for cytochrome *c*. In 1992, Pelletier and Kraut presented the X-ray crystal structure of the complex between yeast cytochrome *c* peroxidase and cytochrome *c* via electrostatic and van der Waals interaction [14]. The active site of cytochrome *c* peroxidase possesses the heme **6**·Fe and coordinated proximal His and a water molecule as axial ligands in the resting state, which is similar to those seen in the myoglobin, although myoglobin lacks the special amino acid groups which support the heterolytic cleavage of the peroxide bond and stabilize the oxoferryl species. Therefore, the present reconstituted myoglobin, rMb(**5**·Fe), having high affinity for cytochrome *c*, would indeed be expected to reveal good peroxidase activity.

Upon addition of H_2O_2, the ferric state of rMb(**5**·Fe) was readily converted to oxoferryl state, whose characteristic absorption band was consistent with that of compound II-like ferryl species derived from native myoglobin Mb(**6**·Fe). Decay of ferrocytochrome *c* absorbance at 550 nm in Fig. 7 indicates the catalytic oxidation of ferrocytochrome *c* by use of rMb(**5**·Fe) or Mb(**6**·Fe) in the presence of H_2O_2. Compared to native myoglobin, the reconstituted myoglobin resulted in the acceleration of the oxidation of ferrocytochrome *c* in the presence of H_2O_2 and the rates increased with decrease of ionic strength. For example, the oxidation rates based on turnover frequency are determined to be 2.1×10^{-2} s^{-1} for rMb(**5**·Fe) and 3.2×10^{-3} s^{-1} for Mb(**6**·Fe), respectively, in 5 mM phosphate buffer at 20°C [17]. These results indicate that complex formation between the reconstituted myoglobin and cytochrome *c* accelerates the oxidation of ferrocytochrome *c* in a similar manner to the cytochrome *c* peroxidase–cytochrome *c* complex.

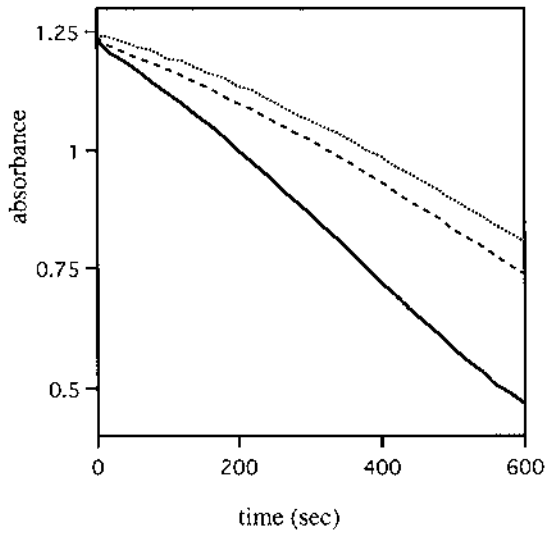

Fig. 7. Decay of ferrocytochrome *c* (4.5×10^{-5} M) catalyzed by myoglobin (1.5×10^{-6} M) in the presence of H_2O_2 (3.6×10^{-4} M) in 5 mM phosphate buffer (pH 7.0) at 20°C. Solid line corresponds to reconstituted myoglobin rMb(**5**·Fe); dashed line corresponds to native myoglobin Mb(**6**·Fe); dotted line corresponds to control experiment in the absence of myoglobin. The decay was monitored at 550 nm.

5. Conclusions

Over the last decade, there has been a large body of literature exploring the modification of hemoprotein by use of the site-directed mutagenic approach or nonselective chemical modification of amino acid residue of the protein. However, to date, the studies aimed at the functionalization of the protein based on heme modification have been quite limited [18,19]. The achievement of such a stable diprotein complex formed by electrostatic interaction may thus serve as a new way for the future design of artificial protein–protein complexes, which will provide insights into the biological mechanism of interfacial recognition and reaction through the protein surface.

References

[1] B. Durham, F.S. Millett, in: K.S. Suslick (Ed.), Comprehensive Supramolecular Chemistry, vol. 5, Oxford, 1996, p. 219.
[2] (a) S. Iwata, C. Ostermeier, B. Ludwig, H. Michel, Nature 376 (1995) 660. (b) T. Tsukihara, H. Aoyama, E. Yamashita, T. Tomizaki, H. Yamaguchi, K. Shinzawa-Itoh, R. Nakashima, R. Yaono, S. Yoshikawa, Science 269 (1995) 1069.
[3] T. Hayashi, H. Ogoshi, Chem. Soc. Rev. 26 (1997) 355.
[4] F.W. Teale, Biochim. Biophys. Acta 35 (1959) 543.

[5] T. Hayashi, T. Takimura, Y. Aoyama, Y. Hitomi, A. Suzuki, H. Ogoshi, Inorg. Chim. Acta 275-276 (1998) 159.
[6] T. Hayashi, T. Takimura, H. Ogoshi, J. Am. Chem. Soc. 117 (1995) 11606.
[7] T. Hayashi, A. Tomokuni, T. Mizutani, Y. Hisaeda, H. Ogoshi, Chem. Lett. (1998) 1229.
[8] S.V. Evans, G.D. Brayer, J. Mol. Biol. 213 (1990) 885.
[9] N. Mataga, A. Karen, T. Okada, S. Nishitani, N. Kurata, Y. Sakata, S. Misumi, J. Phys. Chem. 88 (1984) 5138.
[10] (a) N. Barboy, J. Feitelson, Biochemistry, 28 (1989) 5450. (b) J. Feitelson, G. McLendon, Biochemistry 30 (1991) 5051. (c) S. Aono, S. Nemoto, I. Okura, Bull. Chem. Soc. Jpn. 65 (1992) 591. (d) K. Tsukahara, M. Okada, S. Asami, Y. Nishikawa, N. Sawai, T. Sakurai, Coord. Chem. Rev. 132 (1994) 223.
[11] Y. Hitomi, T. Hayashi, H. Ogoshi, J. Inorg. Biochem. 67 (1997) 113.
[12] T. Hayashi, Y. Hitomi, H. Ogoshi, J. Am. Chem. Soc. 120 (1998) 4910.
[13] (a) S.J. Moench, S. Chroni, B.-S. Lou, J.E. Erman, J.D. Satterlee, Biochemistry 31 (1992) 3661. (b) Q. Yi, J.E. Erman, J.D. Satterlee, Biochemistry 32 (1993) 10988.
[14] H. Pelletier, J. Kraut, Science 258 (1992) 1748.
[15] J.M. Nocek, B.P. Sishta, J.C. Cameron, A.G. Mauk, B.M. Hoffman, J. Am. Chem. Soc. 119 (1997) 2146.
[16] K. Tsukahara, C. Kimura, J. Electroanal. Chem. 438 (1997) 67.
[17] T. Hayashi, Y. Hitomi, T. Ando, T. Mizutani, Y. Hisaeda, S. Kitagawa, H. Ogoshi, J. Am. Chem. Soc. 121 (1999) in press.
[18] T. Hayashi, T. Takimura, T. Ohara, Y. Hitomi, H. Ogoshi, J. Chem. Soc. Chem. Commun. (1995) 2503.
[19] I. Hamachi, Y. Tajiri, T. Nagase, S. Shinkai, Chem. Eur. J. 3 (1997) 1025.